EFFECT OF STATOR AND ROTOR POLE SHAPES ON THE TORQUE RIPPLE IN A SWITCHED RELUCTANCE MOTOR

Yusuf OZOGLU
Vocational Sch. of High Tech,
University of Istanbul, 34850, Avcılar, İstanbul,
Tel: (0212) 5911079,
e-mail: yozoglu@istanbul.edu.tr

Nurdan GUZELBEYOGLU
Electrical Eng. Dept.,
Istanbul Technical University., 80626, Maslak, Istanbul,
Tel:(0212) 2856742,
e-mail: nurdan@elk.itu.edu.tr

***Abstract** – Switched Reluctance Motor (SRM) has high torque ripple which is undesiable. In this paper, the effects of new stator and rotor shapes on the torque ripple have been examined by using finite element method (FEM) and the model providing the lowest torque ripple has been proposed.*

1.INTRODUCTION

In recent years, there has been a growing interest in the design, control and application of switched reluctance motor (SRM). SRM has been used in many industrial applications such as low-power servomotors and high-power traction drives, just because of its simplicity and controllability. However, SRM produces high torque ripple when phase windings are excited sequentially. High torque ripple cause acoustic noise and damage to the bearings and therefore is to be reduced to acceptable level.

There are two basic methods to reduce the torque ripple of SRM: 1- the method dealing with magnetic design of motor [1-4], 2- the method using design of control circuit of motor [5-8]. In this paper, the first method has been studied. Using the ANSYS package program, finite element method (FEM) has been applied to SRM and nonlinear magnetic analysis has been performed [9].

2.FINITE ELEMENT MODEL OF THE SRM

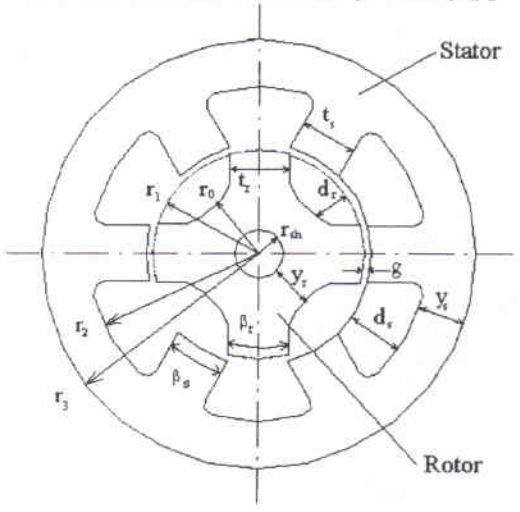

Figure 1. The geometry of 6/4 SRM

The examined model of the switched reluctance motor is 3-phase, 6/4 motor, which has 6 stator and 4 rotor poles [10]. The whole geometry of SRM is shown in Figure 1 and the values of the geometric parameters are given in Table 1. Each phase winding is placed on diagonally opposite stator poles. There is no winding on rotor poles. Exciting voltage of motor winding is 24 V (dc), other nominal values of the motor are 11 A (current), 1.25 Nm (torque) and 261 W (shaft power).

Table 1. Values of geometric parameters

Parameter	Value
r_0	$0.1734 \cdot 10^{-1}$ m
r_1	$0.2349 \cdot 10^{-1}$ m
r_2	$0.3881 \cdot 10^{-1}$ m
r_3	$0.4699 \cdot 10^{-1}$ m
t_s	$0.1226 \cdot 10^{-1}$ m
t_r	$0.1295 \cdot 10^{-1}$ m
d_s	$0.1508 \cdot 10^{-1}$ m
d_r	$0.6147 \cdot 10^{-2}$ m
y_s	$0.8179 \cdot 10^{-2}$ m
y_r	$0.8636 \cdot 10^{-2}$ m
g	$0.2286 \cdot 10^{-3}$ m
β_s	30°
β_r	32°

First of all, finite element model of SRM has been built to obtain behavior of SRM. For this reason, solid modeling of SRM has been designed by using the geometric parameters in the computer. Material properties defined as BH magnetizing curve are shown in Figure 2. Since the core material of SRM has nonlinear properties, the model of SRM has also nonlinear characteristics. The winding regions of the model have been defined taking electrical resistivity as ρ=1.922·10-8 [Ω·m].

The element defined by eight nodes for 2-D model has been used in the finite element model of SRM. The element of a higher-order has nonlinear magnetic capability for modeling B-H curves. Element type has three degrees of freedom per node: magnetic vector potential (AZ), current (CURR), electromotive force (EMF) [9].

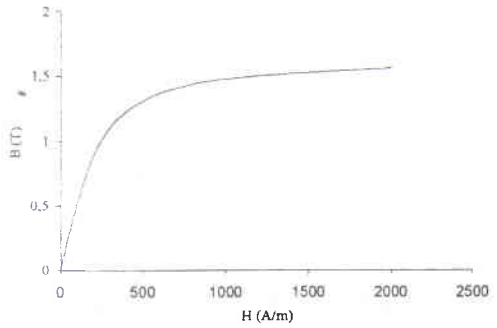

Figure 2. Magnetizing curve of the core materials

The whole model has been discretized by the elements. Modelling in the air gap of SRM is very important and several layers of elements may be required to obtain a good field solution. The air gap ($g=0.2286\cdot10^{-3}$ m) between the radial pair of stator and rotor poles has been finely discretized in four layers. The finite element model of SRM consist of approximately 6000 elements and 16000 nodes.

The magnetic field of SRM is governed by the 2-dimensional nonlinear Poisson equation [9]:

$$\frac{\partial}{\partial x}\left(\nu\frac{\partial A_z}{\partial x}\right)+\frac{\partial}{\partial x}\left(\nu\frac{\partial A_z}{\partial y}\right)=-J_o \qquad (1)$$

A_z : z-component of the vector potential, A,

ν : magnetic reluctivity,

J_o : z-component of the current density, J.

The finite element method is used to obtain the magnetic vector potential values throughout the motor. These vector potential values can be processed to obtain the field distribution, flux linkage and torque. The static analysis has been performed using the finite element model of SRM. The solution includes neither time nor the velocity vector.

3.CALCULATION OF TORQUE CHARACTERISTIC

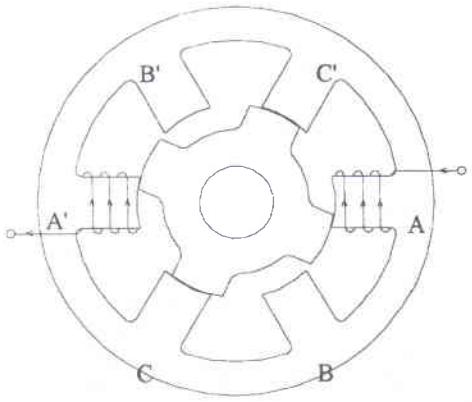

Figure 3. A phase winding of 6/4 SRM

The SRM is sequentially excited from the stator windings wound in series on diagonally opposite stator poles. Only one of the three-stator phase winding is shown in Figure 3. For motoring operation, a stator phase winding must be excited when the interpolar axis of the rotor is aligned with the stator pole and must be turned off before rotor pole is exactly aligned with the stator pole.

Continuous rotation of the rotor is achieved by exciting the stator phase windings sequentially. The direction of the torque is always towards the nearest aligned position. Therefore, positive torque (motoring torque) can be produced only if the rotor is between the unaligned position and the next aligned position in the forward direction (Fig. 4.).

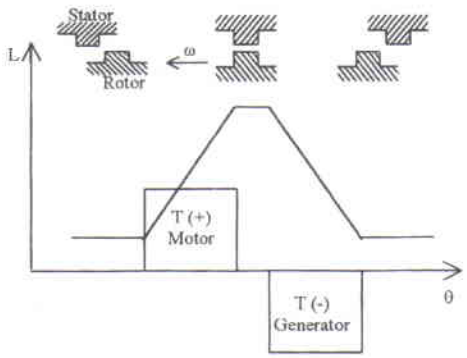

Figure 4. Inductance and torque curves of SRM

In a non-saturable motor, the torque equation can be written as [10]:

$$T=\frac{1}{2}\frac{\partial L}{\partial\theta}i^2 \qquad (2)$$

L : inductance of the stator winding,

θ : rotor position,

i : phase current.

The inductance curve $L(\theta)$ for the non-saturable motor is shown in Fig. 4. During the period of overlap $dL/d\theta$ is constant, so the torque will be constant if the current held constant during this period. When the sequence of excited phase is changed, the torque ripple does not occur. Whereas for a saturable motor, passing from one phase to the next phase causes the torque ripple. The torque ripple of SRM is an important problem as if causes acoustic noises and damage to bearing of SRM.

Maxwell-Stress tensor method is used to calculate the torque characteristic. In 2-D model of SRM, the total torque developed can be written as [9]:

$$T=\nu_0 ZR\int_s B_r\cdot B_\theta dS \qquad (3)$$

ν_0 : reluctivity of air,

Z : length of SRM,

R : radius of cylindrical surface in the middle of airgap,

B_r : radial component of the flux density,

B_θ : tangential component of the flux density.

The torque developed in the static solution can be called as static torque characteristic of SRM. The static torque characteristic of SRM has been obtained over an angular displacement range from 0° to 45° for winding excitation currents of 3, 5, 7, 10, 15 and 20 A. The rotor pole was rotated in 5° increments and the winding was excited by current. Then the torque value has been obtained for each rotor position and for each current level.

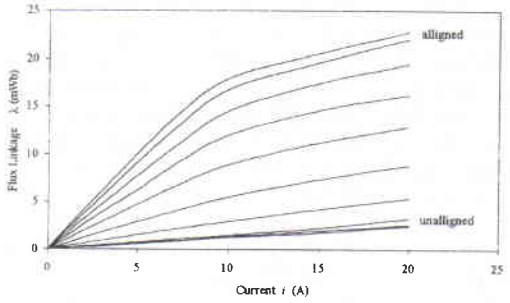

Figure 5. Flux linkage curve of Model 1.

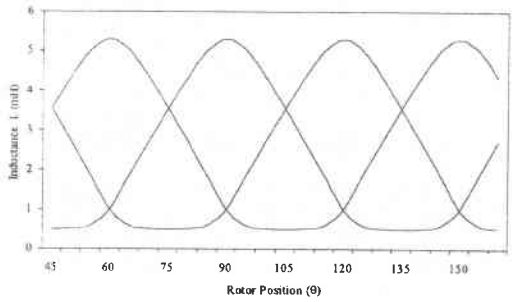

Figure 6. Inductance curve of Model 1 (10 A).

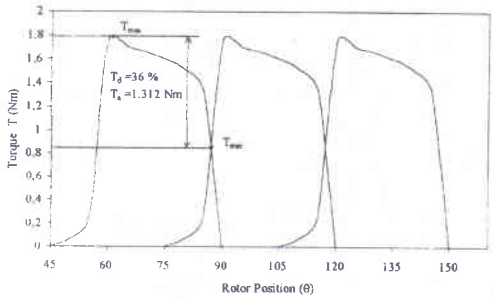

Figure 7. Torque curve of Model 1 (10 A).

Model 1 of SRM which has original pole shapes has been analyzed. Under the saturable condition, the flux linkage, inductance and the torque curves of Model 1 has been obtained as shown in Fig. 5,6 and 7.

The ratio of the torque ripple can be calculated as shown below:

$$T_d\,\% = \frac{\Delta T}{T_a} \times 100 = \frac{T_{max} - T_{min}}{T_{max} + T_{min}} \times 100 \qquad (4)$$

ΔT : the half of difference between max. and min. values of the torque.

T_a : the average value of the torque,

T_{max} : the value which the torque curve reaches the maximum,

T_{min} : the value which the two torque curves cut each other.

The torque has been obtained for all current levels but only compared with other Model's torque under nominal condition (10 A). The ratio of the torque ripple for Model 1 has been calculated as T_d=36 % under the saturable condition and nominal working. This is a very high ratio and must be minimized by changing the stator and rotor pole shapes as proposed below. The average value of the torque was obtained as T_a=1,312 Nm for Model 1.

4.NEW STATOR AND ROTOR POLE SHAPES PROPOSED

To minimize the torque ripple shown in Fig. 7., torque drop must be prevented in the region between T_{max} and T_{min}, while keeping the average torque value within acceptable limits.

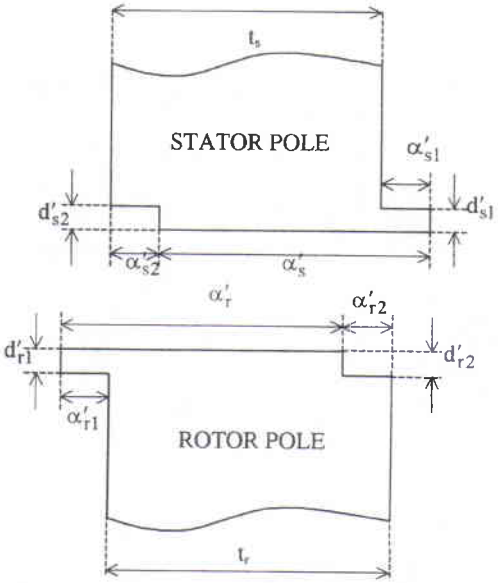

Figure 8. The new parameters defined on the poles.

As a prerequisite for changing torque curve to reduce torque ripple inductance curve must be changed. Stator and rotor pole shapes are among the factors affecting inductance curve and therefore must be duly changed. New geometric parameters on the stator and rotor pole tips have been defined as shown in Fig .8. Five models (M2, ..., M6) with different stator and rotor pole shapes have been obtained by changing these parameters, as listed in Table 2.

Table 2. New geometric parameters defined on the stator and rotor poles for new models.

	M2	M3	M4	M5	M6
β_{s1}'	4g	2g	4g	4g	4g
d_{r1}'	4g	2g	4g	4g	4g
d_{s2}'	2g	2g	2g	2g	2g
d_{r2}'	2g	2g	2g	2g	2g
α_s'	30°	30°	30°	30°	31°
α_r'	32°	32°	32°	32°	33°
α_{s1}'	5°	6°	6°	4°	5°
α_{r1}'	5°	6°	6°	4°	4°
α_{s2}'	5°	6°	6°	4°	5°
α_{r2}'	5°	6°	6°	4°	4°
T_d %	14.3	44.8	38.5	27.7	11.9
T_a	1,377	1,087	1,137	1,272	1,362

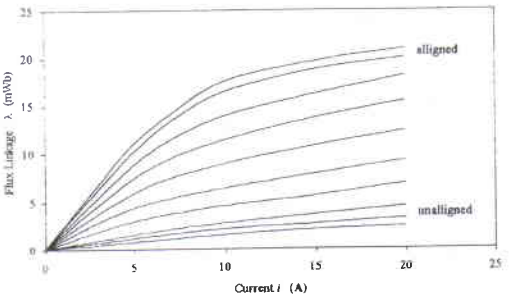

Figure 9. Flux linkage curve of Model 6.

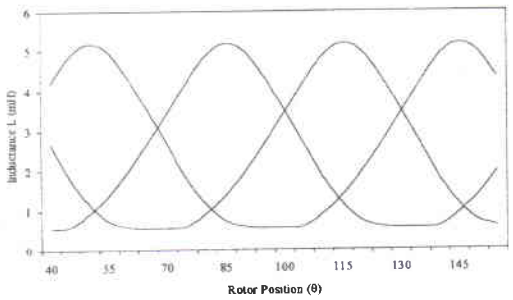

Figure 10. Inductance curve of Model 6 (10 A).

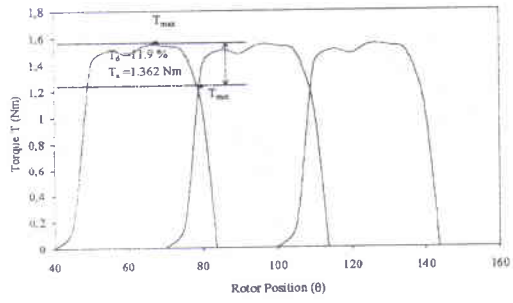

Figure 11. Torque curve of Model 6 (10 A).

As can be concluded from Table 2. Model 6 is the best one from the viewpoint of torque ripple (T_d=11.9 %), while the average torque has remained almost constant. Under saturable condition, the flux linkage, inductance and the torque curves of Model 6 have been obtained as shown in Fig. 9,10 and 11.

Remember that Model 1 with classical pole shapes had a ripple of T_d=36 %. When compared with this figure, the improvement on the torque ripple achieved by Model 6 is 24.1 %. Model 6 is therefore proposed by us to minimize the torque ripple.

5.CONCLUSIONS

Stator and rotor pole shapes are the parameters that affect the torque ripple of SRM. In this paper, new parameters have been introduced into the problem and by changing these parameters five model with different pole shapes have been defined. Then the torques of these five models have been examined and the model having the lowest torque ripple has been proposed. By using this model 24.1 % improvement in the torque ripple has been achieved without any decrease in the average moment.

6.REFERENCES

[1] Schramm, D.S., Williams, B.W., Green, T.C., 1992. Torque Ripple Reduction of Switched Reluctance Motors by Phase Current Optimal Profiling, *PESC'92 Conference,* pp 857-860.

[2] Rochford, C., Kavanagh, R.C., Egan, M.G., and Murphy, J.M.D., 1993. Development of Smooth Torque in Switched Reluctance Motors Using Self-Learning Techniques, *European Power Electronics.*, pp 14-19.

[3] O'donovan, J.G., Roche, P.J., Kavanagh, R.C., Egan, M.G., and Murphy, J.M.D., 1994. Neural Network Based Torque Ripple Minimisation in a Switched Reluctance Motor, *IECON'94 Conf.*, pp 1126-1231.

[4] Ozbulur, V., Bilgic, M., O., Sabanovic, A., 1995. Torque Ripple Reduction of a Switched Reluctance Motor, *IEEE-IPEC 95 Conf.,* Yolohama, JAPAN, pp.567-550

[5] Moallem, M., Ong, C.M., and Unnewehr, L.E., 1992. Effect of Rotor Profiles on the Torque of a Switched Reluctance Motor, *IEEE Trans. on Ind. App.*, Vol. 28, No. 2, pp 364-369.

[6] Le Chenadec, J.Y, Geoffroy, M., Multon, B., and Mouchoux, L.C., 1994. Torque Ripple Minimisation in Switched Reluctance Motors by Optimisation of Current Wave-Forms and of Tooth Shape With Copper Losses and "V.A. Silicon" Constraints, *ICEM'94 Conf.,* Paris, pp 559-564.

[7] Ohdachi, Y., Kawase, Y., Miura, Y., Hayashi, Y., 1997. Optimum Design of Switched Reluctance Motors using Finite Element Analysis, *IEEE Trans. on Magnetics.*, Vol. 33, No. 2, pp 2033-2036.

[8] Koibuchi, K., Ohno, T., and Sawa, K., 1997. a Basic Study for Optimum Design of Switched Reluctance Motor by Finite Elemant Method, *IEEE Trans. on Mag.*, Vol. 33, No:2, pp 2077-2080.

[9] Ansys Inc., ANSYS Theory Manual – Revision 5.4, 1997.

[10] Miller, T. J. E., 1993. Switched Reluctance Motors and Their Control. Oxford University Press, Oxford. airgap.